



Welcome to Busan
SMiRT 24

Transactions, SMiRT-24
BEXCO, Busan, Korea - August 20-25, 2017
Division VI



SEISMIC ISOLATION OF A NUCLEAR STRUCTURE: IMPACTS ON CONSTRUCTION COST AND SEISMIC RISK

Ching-Ching Yu¹, Chandrakanth Bolisetti², Benjamin Kosbab³, Justin Coleman⁴, and Andrew Whittaker⁵

¹ Ph.D. candidate, Department of Civil, Structural, and Environmental Engineering, University at Buffalo, Buffalo, NY, USA

² Research Scientist, Seismic Research Group, Idaho National Laboratory, Idaho Falls, ID, USA

³ Principal Engineer, SC Solutions, Atlanta, GA, USA

⁴ Team Lead, Seismic Research Group, Idaho National Laboratory, Idaho Falls, ID, USA

⁵ Professor and MCEER Director, Department of Civil, Structural, and Environmental Engineering, University at Buffalo, Buffalo, NY, USA

ABSTRACT

Base isolation will substantially reduce horizontal seismic demands in structures, systems and components (SSCs) in nuclear facilities, thus providing opportunities to increase seismic safety and reduce construction cost. Although past studies have characterized the benefits of seismic isolation in terms of increased safety, the possible reductions in construction cost have not been quantified. The over excavation, additional reinforced concrete basemat and the seismic bearings will add to the construction cost, but net savings are possible because the required robustness (and thus cost) of the SSCs is much smaller. Some of these issues are explored using a Generic Nuclear Facility (GNF). Nonlinear dynamic analysis of the GNF is performed for the conventionally founded GNF and an isolated variant of the GNF, for the low-to-moderate seismic hazard site of the Idaho National Laboratory and the high seismic hazard site of the Los Alamos National Laboratory. The building is populated with components routinely found in nuclear facilities, and for which fragility data are available. Analysis is performed per ASCE 4-16 to size the seismic isolators. Seismic risk calculations are performed using seismic probabilistic risk assessment methodology proposed by Huang et al. Two procedures are used to assess system functionality: a simplified method based on Boolean algebra and probability theory, and a rigorous Monte Carlo procedure. The cost to construct the GNF is reduced at both sites when isolation is implemented, with greater savings at the LANL site. The simplified method for assessing system functionality provides reliable estimates of risk and is suitable for use in the early stages of nuclear facility design.

INTRODUCTION

The implementation of seismic isolation in a nuclear facility has four potential benefits: 1) *economic*: reduction in capital cost, 2) *increased safety*: reduction in the mean annual frequency of unacceptable performance, 3) *insurance*: protection against increases in the known seismic hazard after construction by minimizing the effort to re-qualify and re-certify structures, systems and components, and 4) *recertification*: the opportunity to certify an existing NPP design for a region of higher seismic hazard. The *safety* benefit has been addressed in prior studies (e.g., Huang 2011a, 2011b) whereas the *economic* benefit is still unclear. The safety and economic benefits are explored in this study for an archetype building, described hereafter as a Generic Nuclear Facility (GNF).

To generalize the results of the study, two sites of different seismic hazard are considered: 1) the Idaho National Laboratory (INL) in Idaho Falls, ID: low-to-moderate seismic hazard, and 2) the Los Alamos National Laboratory (LANL) in Los Alamos, NM: high seismic hazard. Nonlinear dynamic analysis of numerical models of the GNF is performed in LS-DYNA (LSTC, 2013) for two boundary

conditions: conventionally founded and base-isolated. Seismic hazard calculations are performed for the two sites. Ground motion time series are generated for the dynamic analysis using results of the seismic hazard calculations.

The GNF is assumed to store materials at risk (MAR) and so structures, systems and components (SSCs) that are common to safety-related nuclear structures are used to populate the facility for risk calculations. The base-isolated building is designed to have a translational period of approximately 2 seconds but the design is *not optimized* to minimize either risk or cost. The same isolation system is used at both the INL and LANL sites, resulting in different isolated periods.

Seismic demands on SSCs are generated for both the conventionally founded and base-isolated buildings to investigate the benefit of isolation in terms of reduced risk. The seismic probabilistic risk assessment (SPRA) methodology proposed by Huang et al. (2011a, 2011b) is used for the risk calculations because it can accommodate highly nonlinear soils, isolators and structures. Two procedures are used as part of the SPRA to assess system functionality: 1) a simplified procedure based on Boolean algebra and probability theory and 2) the rigorous Monte Carlo procedure described in Huang et al. (2011a, 2011b) and identified in ASCE/SEI Standard 4-16 (ASCE 2016). Only the effects of horizontal shaking are considered here because fragility curves for the assumed SSCs in the GNF are by-and-large independent of the effects of vertical shaking. Soil-structure-interaction (SSI) analysis is not performed. The data of Stevenson (1981, 2003) are used to estimate 1) overnight capital cost (OCC) and 2) cost of SSCs for the conventionally founded and base-isolated buildings at both sites. (More modern cost data is not publically available.) Detailed information on the study can be found in Bolisetti et al. (2016) and Yu et al. (2017).

DESCRIPTION OF THE FACILITY AND THE ISOLATION SYSTEM

The GNF is a two-story reinforced concrete building founded on a 5-ft. thick basemat. The thickness of its reinforced concrete walls ranges between 1 ft. and 3 ft. The building's plan dimensions are 65 ft. × 160 ft. At its highest point, the building is approximately 38 ft. tall. The total weight of the building, including the basemat, but excluding SSCs, is 21,280 kips. The building is modeled using the finite element code LS-DYNA (LSTC, 2013). Figure 1 presents the finite element model of the GNF, identifying the global coordinate system (X, Y, Z) and representative dimensions. The structural components were assigned linear elastic material properties consistent with those of concrete. The seismic (reactive) weight of 22,845 kips is taken as the dead load and one half of the live load (200 lb/ft² on the slabs and basemat, and of 100 lb/ft² on the roofs). Table 1 presents summary information on the modal properties of the LS-DYNA model, including the seven modes with much of the modal effective mass (MEM) in each horizontal direction. The frequencies of the translational modes are between 20 Hz and 33 Hz in X direction and between 10 Hz and 39 Hz in Y direction.

To populate the building for risk calculations, 8 sample SSCs are chosen from EPRI (2013), including 1) motor control center (MCC), 2) battery, 3) coolant pump, 4) air handler, 5) heating,

Table 1. Modal properties of the LS-DYNA model, ordered by modal effective mass (MEM)

X direction				Y direction			
Mode	Period (sec)	Frequency (Hz)	MEM (%)	Mode	Period (sec)	Frequency (Hz)	MEM (%)
5	0.047	21.3	24	4	0.050	20.0	40
6	0.042	23.8	14	3	0.051	19.6	19
9	0.037	27.0	10	5	0.047	21.3	8
7	0.042	23.8	7	11	0.036	27.8	4
12	0.035	28.6	6	7	0.042	23.8	2
16	0.03	33.3	6	20	0.026	38.5	2
4	0.05	20.0	5	1	0.099	10.1	2

ventilation, air conditioning (HVAC) duct, 6) structure (surrounding the pressure vessel), 7) pressure vessel, and 8) piping. (The numbers are used later in this paper to identify the SSCs in the fault tree.) The nodes and locations of the SSCs are presented in Figure 2.

Thirty-eight lead rubber (LR) bearings are used to isolate the GNF. The *target* isolation period is approximately 2 seconds for design basis shaking (DBE), with the same system being used at both sites. (The isolated period at the LANL site is greater than at the INL site because the seismic hazard is greater at LANL thus producing greater DBE horizontal displacements and corresponding axial forces, and a smaller effective horizontal stiffness.) The isolators are located beneath the shear walls; their spacing is limited to 25 ft. The seismic isolation system was designed for design basis earthquake (DBE) shaking (see next section) per the provisions of ASCE/SEI Standard 4-16 (ASCE 2016). The product of the analysis was one size of isolator for both the INL and LANL sites: 33 inches in diameter, central lead plug of 6 inches in diameter, twenty-five layers of 0.42-inch thick rubber, twenty-four 0.2-inch thick shim plates, two 1.25-inch diameter end plates, and two 1.25-inch thick flange plates, for a total bearing height of 20 inches. The locations of the isolators and their design were *not optimized*.

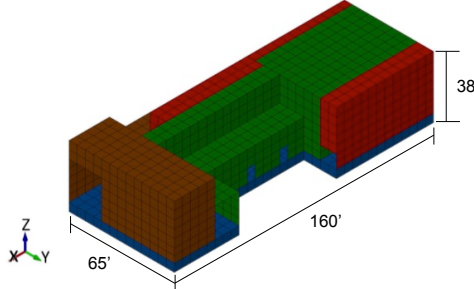


Figure 1. Model of the GNF

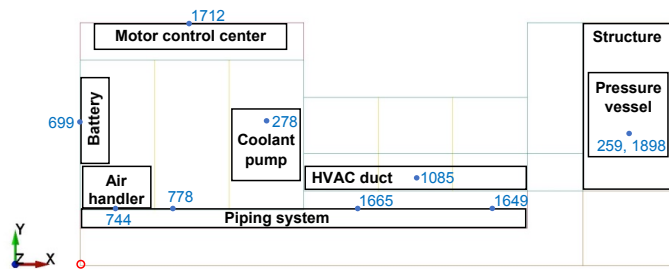


Figure 2. Plan view of the GNF with locations and nodes of SSCs

These 38 LR isolators were modeled using *MAT_SEISMIC_ISOLATOR (197) available in LS-DYNA. The mechanical properties of each isolator are: elastic stiffness (K_e) of 38 kip/in, post-yield stiffness (K_d) of 8.2 kip/in, a characteristic strength (Q_d) of 30 kips. Chapter 12 of ASCE 4-16 requires the calculation of the 80%-ile lateral displacement of the isolation system for DBE shaking and the 90%-ile lateral displacement for 150% DBE shaking (assumed to represent Beyond Design Basis Earthquake (BDBE) shaking.). Sizing of this LR isolator is controlled by the results of analysis for 150% DBE shaking at LANL site: the 90%-ile BDBE displacement of 13.9 inches and the corresponding maximum axial compressive force of 913 kips (maximum of all 38 isolators) are much less than the rated displacement capacity of 22 inches at a maximum axial compression of 1,100 kips: see <http://www.dsi-inc.com/technical.html>, accessed on June 1, 2016.

SEISMIC HAZARD AND GROUND MOTION TIME SERIES GENERATION

To enable generalization of the outcomes from the study to a wide range of new-build nuclear facilities in the United States, isolation systems, risk calculations and cost estimates were prepared for two sites: 1) the Idaho National Laboratory (INL) in Idaho Falls, ID, assumed to represent a site of low-to-moderate seismic hazard, and 2) the Los Alamos National Laboratory (LANL) in Los Alamos, NM, assumed to represent a site of high seismic hazard. Seismic hazard data for INL and LANL were developed using the ground motion calculator at the website of the United States Geological Survey (USGS, <https://geohazards.usgs.gov/hazardtool/application.php>, accessed on June 1, 2016). Subsurface soil at the two sites is assumed to be at the boundary of site classes B and C per ASCE/SEI Standard 7-10 (ASCE 2010). Figure 3a (Figure 3b) presents the seismic hazard curves at periods of 0.1 second (representative of the conventionally founded GNF) and 2 seconds (representative of the isolated GNF) at INL (LANL).

Uniform hazard acceleration response spectra corresponding to a mean annual frequency of exceedance (MAFE) of 10^{-4} for the two sites are generated for horizontal shaking, and these are used to

represent design basis earthquake (DBE) shaking. The target DBE horizontal acceleration response spectrum at INL (LANL) for 5% damping is presented in Figure 4a (Figure 4b), together with thirty sets of two-horizontal-component spectra of maximum direction-minimum direction (max-min) ground motions (Huang et al. 2009) matched collectively to the target spectrum (red line). The seed motions are matched using the time-domain procedure of RSPMatch2005 (Hancock et al. 2006). The seeds are taken from the Pacific Earthquake Engineering Research (PEER) ground motion database (<http://ngawest2.berkeley.edu/>, accessed on June 1, 2016).

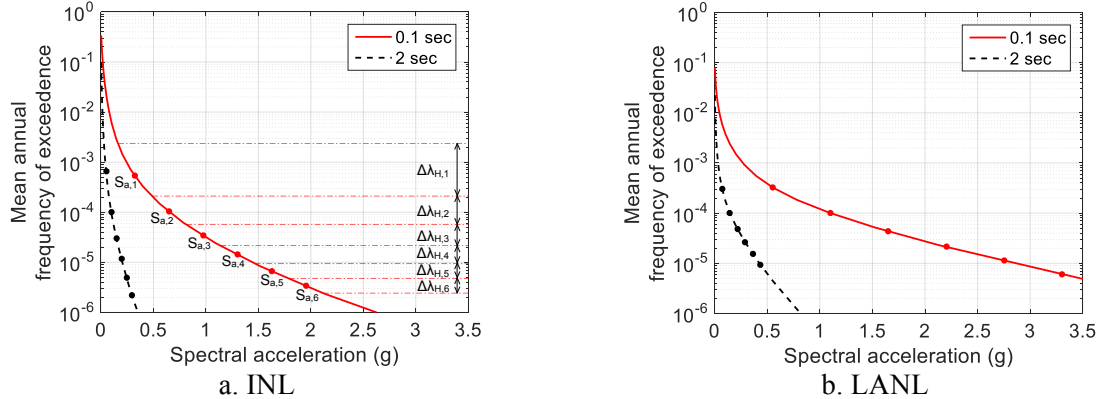


Figure 3. Seismic hazard curves for 5% damping at 0.1 second and 2.0 seconds at INL and LANL

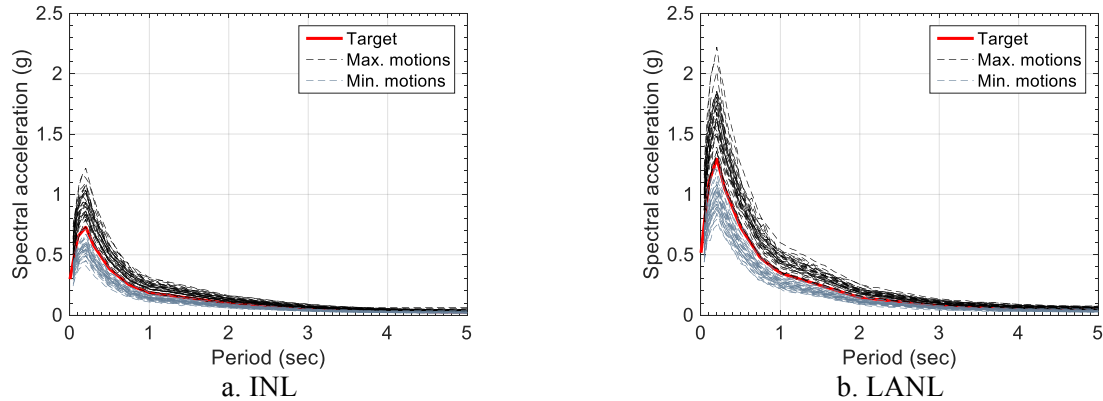


Figure 4. Acceleration response spectra for max-min ground motions, 5% damping: DBE shaking

SEISMIC RISK CALCULATIONS

Seismic probabilistic risk assessment (SPRA) is used to compute the mean annual frequency of unacceptable performance, which would include core damage and large early radiation release for the existing fleet of commercial nuclear power plants in the United States. The SPRA methodology used in this study is that proposed by Huang et al. (2011a, 2011b), which was developed to accommodate nonlinear elements in a soil-facility system, including nonlinear soils and seismic isolators. The Huang SPRA methodology involves five steps: 1) perform plant system analysis, 2) characterize seismic hazard and generate ground motion time series, 3) simulate seismic response of SSCs, 4) assess system functionality, and 5) calculate risk.

Step 1: Plant system analysis

The GNF is assumed to store materials at risk (MAR). A highly simplified, hypothetical event tree is assumed for this system. The event tree is presented in Figure 5, which shows that MAR will be lost to the atmosphere if the system fails in an earthquake. A hypothetical fault tree for this system is

presented in Figure 6, including the 8 assumed SSCs binned into 3 categories: confinement, mechanical, and electrical components. The notation \square (AND) and \triangle (OR) gates in Figure 6 describe the assumed path (and resistance) to a loss of MAR. Failure of a component/event immediately above an AND gate requires failure of all the components/events immediately below the gate. The failure of a component/event immediately above an OR gate requires failure of one or more components/events immediately below the gate. The system is assumed to have failed if 1) confinement is lost, 2) mechanical components fail, or 3) electrical components fail.

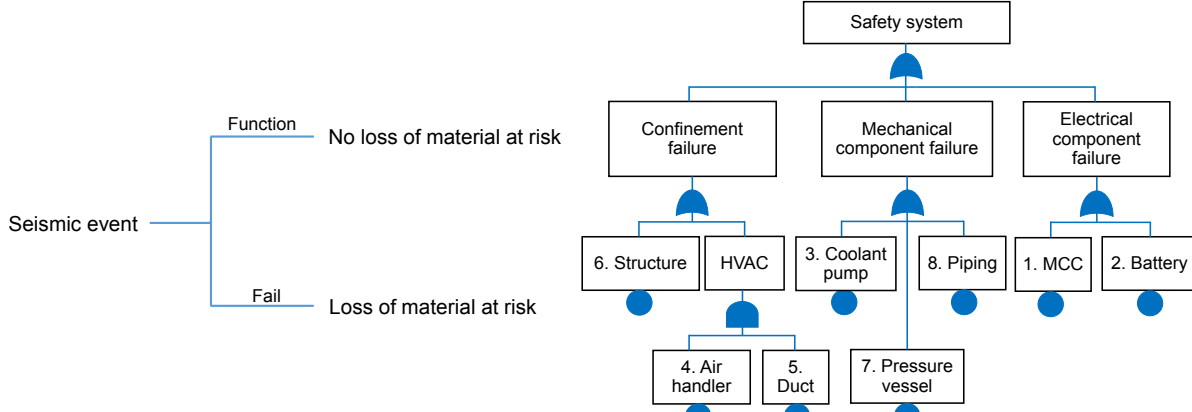


Figure 5. Event tree

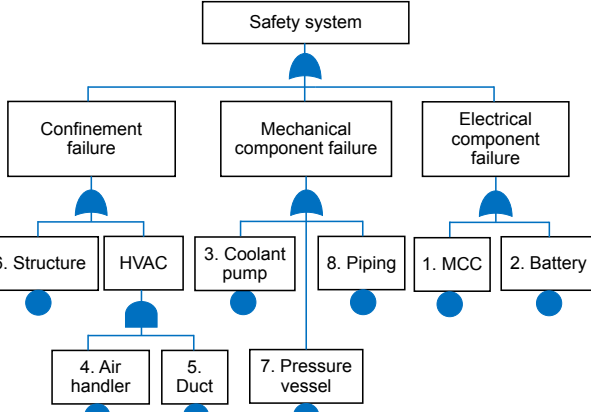


Figure 6. Fault tree

The risk calculations performed in this study use fragility curves characterized using local responses (e.g., average floor spectrum acceleration at the point of attachment) because demands on SSCs are calculated directly by response-history analysis. Fragility curves for the SSCs are developed assuming lognormal distributions using appropriate demand parameters (see Bolisetti et al., 2016; Yu et al., 2017). Mean composite fragility curves, as proposed by Reed and Kennedy (1994), are used here:

$$P_f(a) = \Phi\left[\frac{\ln(a/\hat{a})}{\beta_c}\right] \quad (1)$$

where $P_f(a)$ is the probability of failure of the component at a demand of a . Parameter \hat{a} is the median (50%-ile) value of the capacity of the component. The logarithmic standard deviation, β_c , of the curve is a composite parameter combining aleatory variability (or randomness), β_r , which is inherent in the variable a , and epistemic uncertainty, β_u , associated with a lack of knowledge, and calculated as:

$$\beta_c = \sqrt{\beta_u^2 + \beta_r^2} \quad (2)$$

EPRI (2013) proposes generic values for β_u and β_r for peak ground acceleration- (PGA-) based fragility curves for SSCs in nuclear structures. Although the values of β_u and β_r for PGA-based fragility curves include uncertainty in structure response, those values are used to calculate β_c in this study because 1) more directly applicable values are not readily available, and 2) the use of these values should not bias the relative risk in the conventionally founded and isolated GNF.

The value of a associated with a 95% confidence of a 5% failure probability is defined as the high-confidence-of-low-probability (HCLPF) capacity. The median \hat{a} can then be calculated by:

$$\hat{a} = HCLPF \cdot e^{1.65(\beta_r + \beta_u)} \quad (3)$$

For this study, the HCLPF capacities for the 8 SSCs are attached to the median responses of the conventionally founded structure at their points of attachment, calculated by analysis using the 30 DBE ground motions. This was done to ensure that the component fragilities are *reasonably* consistent with minimum expected seismic performance in the United States. Identical SSCs are used in both the conventionally founded and base-isolated buildings for each site, but with different fragility curves at each site because design basis earthquake shaking at LANL is more intense than at INL.

Step 2: Characterize seismic hazard

Hazard analysis is performed at the two sites: INL and LANL. The hazard curves of Figure 3 are divided into 6 intensity intervals. Each interval has a mean annual frequency of occurrence ($\Delta\lambda_i$) and a mid-point spectral acceleration ($S_{a,i}$) for the i th intensity interval identified by the solid red circles (0.1 second) and the solid black circles (2.0 seconds). The parameters $S_{a,i}$ and $\Delta\lambda_i$ are shown only for the 0.1-second hazard curve in Figure 3a, but the same process is applied to both sets of hazard curves. These intensities are decimal fractions of DBE shaking: 0.5DBE, DBE, 1.5DBE, 2DBE, 2.5DBE, and 3DBE. The values of $S_{a,i}$ and $\Delta\lambda_i$ are listed in Table 2 for both sets of hazard curves.

Step 3: Simulate seismic response of SSCs

Thirty pairs of horizontal max-min ground motions time series are scaled to each of the midpoint spectral accelerations and used for response-history analysis of the conventionally founded and base-isolated GNFs at each site. Figure 7 presents in-structure spectra for a frequency range of 2 Hz to 33 Hz, assuming a damping ratio of 2%, at Node 278 (see Figure 2), which is the location of coolant pump. Data are presented in the X and Y directions, for the 30 DBE pairs of ground motions, together with the mean spectrum (blue line for the conventionally founded building and red line for the base-isolated building), for the LANL site. The spectral accelerations in the base-isolated building are much smaller than those in the conventionally founded building, which is an expected result. The demands on the SSCs, as used to define the fragility functions (average or peak spectral acceleration for the frequency range of interest at 2% damping), are calculated and arranged in demand matrices. The size of the demand matrices is 30×8 , where the number of row vectors is determined by the number of nonlinear response-history analyses for a given intensity of shaking and the number of columns is determined by the number of SSCs. Demand matrices are generated for the 6 intensities of shaking, for each GNF at each site.

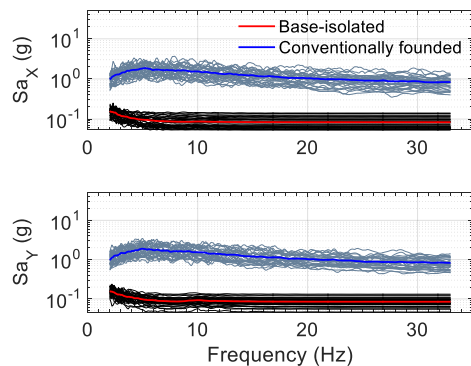


Figure 7. In-structure acceleration response spectra on Node 278, 2% damping, LANL site

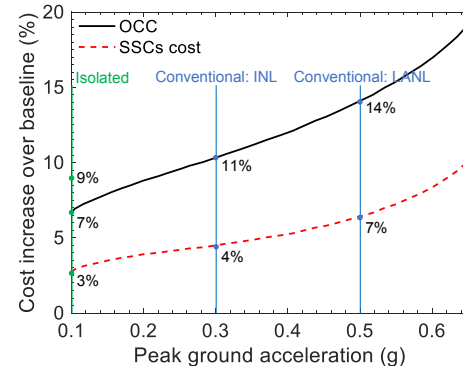


Figure 8. Increase in cost as a percentage of the OCC of the baseline (non-seismic) design

Step 4: Assess system functionality

Two procedures are used here to estimate the probability of unacceptable performance conditioned on an intensity of earthquake shaking: 1) a simplified method based on Boolean algebra and probability theory, and 2) the rigorous Monte Carlo procedure presented in Huang et al. (2011a, 2011b).

Simplified procedure:

The simplified procedure utilizes Boolean algebra and basic probability theory. The failure probability of the components/events in the fault tree can be calculated using the failure probability of each sub-component ($P_{f,i}$, i = the number of component). In the fault tree of Figure 6, assuming independence of components 1 through 8, the failure probability of the HVAC system is ($P_{f,4} \times P_{f,5}$) and

of the electrical component is ($P_{f,1} + P_{f,2} - P_{f,1} \times P_{f,2}$). Thirty values of failure probability are computed for each SSC at each level of shaking using the fragility curve and the demand on the SSC. The Boolean algebra in the fault tree and basic probability theory are used to compute the conditional probability of unacceptable performance for each of 30 nonlinear response-history analyses. The conditional probability of unacceptable performance, $P_{UP}(S_{a,i})$, at the chosen intensity of shaking is the average of the 30 values. The values of $P_{UP}(S_{a,i})$ for the conventionally founded and base-isolated buildings are presented in Table 2 for both sites.

Monte Carlo procedure:

A large number of realizations for each level of earthquake shaking intensity is required for the Monte Carlo procedure. The procedure developed by Yang et al. (2009) and implemented in FEMA P-58 (FEMA, 2012) is used to generate a large numbers of realizations, assuming a lognormal distribution for the demands on the SSCs. The number of the realizations, N , is determined using a procedure proposed by Yu and Huang (2017) to obtain an accurate estimate of the conditional probability of unacceptable performance at each level of shaking. The size of the augmented demand matrices is $N \times 8$. For each SSC, a random number is generated from a uniform distribution between 0 and 1 and compared to its failure probability, $P_{UP}(S_{a,i})$. If the random number is less than or equal to $P_{UP}(S_{a,i})$, the SSC is considered to have failed. Otherwise it is considered to be functional. Boolean algebra in the fault tree is then used to determine whether the performance is acceptable (or not) for the realization. The result from each realization is a Bernoulli random variable since the only outcomes are either *occurrence* or *non-occurrence*. The process is repeated for all realizations in the augmented demand matrix. The conditional probability of unacceptable performance, $P_{UP}(S_{a,i})$, at the chosen intensity of shaking, is then given by:

$$P_{UP}(S_{a,i}) = \frac{n_{UP}}{N} \quad (4)$$

where n_{UP} is the total number of occurrences of unacceptable performance. The values of $P_{UP}(S_{a,i})$ for the conventionally founded and base-isolated buildings are presented in Table 2 for both sites.

Step 5: Seismic risk computation

The seismic risk (or annual frequency of unacceptable performance), λ_{UP} , is the sum of the products of $P_{UP}(S_{a,i})$ and the corresponding $\Delta\lambda_i$, as given in equation (5). The results of the risk calculations are presented in Table 2.

$$\lambda_{UP} = \sum_{i=1}^6 P_{UP}(S_{a,i}) \cdot \Delta\lambda_{H,i} \quad (5)$$

Discussion

The probabilities of unacceptable performance in the base-isolated GNF, at the two lowest intensities of shaking, $S_{a,1}$ and $S_{a,2}$, for the Monte Carlo-based calculations are zero at both sites because many more realizations ($= N$) are required to produce non-zero values. However, these additional realizations are not needed because the results of analysis using the simplified procedure show that the contributions to the total mean annual frequency of unacceptable performance from the two lowest intensities of earthquake shaking are tiny.

The introduction of seismic isolation reduces the mean annual frequency of unacceptable performance by 7 to 8 orders of magnitude regardless of whether the simplified or the Monte Carlo is used for the SPRA. This significant reduction in seismic risk, to levels much smaller than the target performance goals of ASCE/SEI Standard 43-05 (ASCE, 2005), enables a significant reduction in the required seismic ruggedness of the SSCs (and thus the cost of the SSCs) in the GNF.

The simplified procedure produces estimates of risk that are comparable to those computed by the more rigorous Monte Carlo procedure, at a very much lower computational expense. This simplified procedure appears to be an efficient tool for risk calculations in the early phases of the design of a nuclear

Table 2. Midpoint spectral accelerations, $S_{a,i}$, annual frequencies of occurrence, $\Delta\lambda_i$, probabilities of unacceptable performance, $P_{UP}(S_{a,i})$, and risk calculations

a. INL

i	Conventionally founded building			Isolated building				
	$S_{a,i}$ (g)	$\Delta\lambda_i$	$P_{UP}(S_{a,i})$		$S_{a,i}$ (g)	$\Delta\lambda_i$	$P_{UP}(S_{a,i})$	
			Simplified	Monte Carlo			Simplified	Monte Carlo
1	0.33	2.16×10^{-3}	0.011	0.013	0.05	3.19×10^{-3}	4.43×10^{-14}	0
2	0.65	1.54×10^{-4}	0.240	0.233	0.10	1.68×10^{-4}	1.61×10^{-11}	0
3	0.98	3.53×10^{-5}	0.636	0.618	0.15	3.55×10^{-5}	1.09×10^{-9}	1.67×10^{-9}
4	1.30	1.19×10^{-5}	0.878	0.895	0.20	1.12×10^{-5}	1.82×10^{-8}	2.10×10^{-8}
5	1.63	4.78×10^{-6}	0.968	0.973	0.24	4.28×10^{-6}	2.25×10^{-7}	5.16×10^{-7}
6	1.95	2.32×10^{-6}	0.993	0.987	0.29	1.69×10^{-6}	1.36×10^{-6}	3.07×10^{-6}
λ_{UP}		1.01×10^{-4}	1.03×10^{-4}		λ_{UP}		3.50×10^{-12}	7.69×10^{-12}

b. LANL

i	Conventionally founded building			Isolated building				
	$S_{a,i}$ (g)	$\Delta\lambda_i$	$P_{UP}(S_{a,i})$		$S_{a,i}$ (g)	$\Delta\lambda_i$	$P_{UP}(S_{a,i})$	
			Simplified	Monte Carlo			Simplified	Monte Carlo
1	0.55	7.94×10^{-4}	0.007	0.008	0.07	6.97×10^{-4}	6.40×10^{-16}	0
2	1.10	1.04×10^{-4}	0.203	0.207	0.15	9.20×10^{-5}	1.51×10^{-12}	0
3	1.65	3.50×10^{-5}	0.605	0.600	0.22	3.33×10^{-5}	1.53×10^{-10}	1.67×10^{-10}
4	2.20	1.47×10^{-5}	0.861	0.880	0.29	1.55×10^{-5}	3.79×10^{-9}	4.83×10^{-9}
5	2.75	7.21×10^{-6}	0.959	0.957	0.36	8.28×10^{-6}	4.81×10^{-8}	6.48×10^{-8}
6	3.30	3.87×10^{-6}	0.989	0.993	0.44	4.37×10^{-6}	3.57×10^{-7}	4.68×10^{-7}
λ_{UP}		7.09×10^{-5}	7.25×10^{-5}		λ_{UP}		2.02×10^{-12}	2.66×10^{-12}

facility, when data are limited. The infusion of risk calculations into the design process should inform early decision-making to achieve specified target performance goals.

COST STUDY

Consideration of the effects of earthquake shaking substantially increases the cost of nuclear facilities: increased component sizes and ruggedness, compromises to the efficiency of the nuclear and mechanical systems, time and expense to characterize and then analyse and design for earthquake loadings, cost of seismic qualification, and time and expense for regulatory review, for example.

Base isolation substantially reduces seismic demands on SSCs in nuclear facilities. Herein, incremental seismic-related costs are estimated for 1) the overnight capital cost (OCC) of the GNF, and 2) the cost of the SSCs in the GNF, for the conventionally founded and base-isolated buildings, at INL and LANL.

Stevenson's studies of 1981 and 2003, which focused on the cost of building a 1200MW light water reactor power plant, provide the most comprehensive source of data that relates increase in plant cost to the increase in intensity of design basis shaking. (More modern data are not publically available.) Stevenson (1981) binned the total cost of a large light water reactor into 1) site preparation and foundations, 2) building structures, 3) mechanical components, 4) electrical components, 5) distribution systems, and 6) engineering costs. Structures, systems and components were included in bins 2, 3, 4 and 5. Stevenson (2003) reported the percentage increase in the OCC over the baseline, non-seismic, plant cost, as a function of design PGA: see the black solid line in Figure 8. The red dashed line in the figure is an estimate of the increase in cost of the SSCs as a function of design PGA. The design basis PGAs for the INL (= 0.3 g) and LANL (= 0.5 g) sites, and the corresponding percentage increases in cost (OCC and SSC) associated with seismic design and construction, are also shown in the figure. The increases in the

OCC over the baseline of \$550 million USD are 11% and 14%, at the INL and LANL sites, respectively. The corresponding increases in the cost of the SSCs are 4% and 7%.

Structures, systems and components in the base-isolated GNF must also be designed for the effects of earthquake shaking. In Figure 7, the mean peak floor acceleration (taken here as the spectral acceleration at a frequency of 33 Hz) for Node 278, which is located on the basemat above the isolators, in the base-isolated GNF, is less than 0.1 g for LANL site. Smaller responses are expected at the INL site. A value of 0.1 g is used here to characterize the maximum seismic demand on the SSCs in the isolated GNF: the assumed percentage increases in cost mapped from Figure 8 at this spectral acceleration are 3% (SSCs) and 7% (OCC). The costs of the additional design and construction to implement the isolation system (additional excavation, additional reinforced concrete for the foundation and pedestals, and isolators) are estimated to be \$10 million USD, which is approximately 2% of the OCC of the baseline GNF of \$550 million USD. Adding this expense to the cost of the SSCs designed to resist a spectral demand of 0.1 g, results in a 9% increase over the baseline (non-seismic) OCC. The increases in cost over the baseline (non-seismic) associated with considerations of earthquake shaking are reduced by 2% (OCC) and 1% (SSCs) by the use of seismic isolation at INL, and by 5% (OCC) and 4% (SSCs) at LANL.

Anecdotal evidence collected by the authors in the past two years suggests that the seismic cost penalties estimated by Stevenson more than 20 years ago are low, indicating that the economic benefits of implementing seismic isolation would be much greater if contemporary data were used, including those costs associated with seismic qualification of SSCs, project-specific engineering calculations, and regulatory review.

SUMMARY AND CONCLUSIONS

This study provides a framework for assessing the benefits of seismic isolation and exercises the framework on a GNF. The two potential benefits of seismic isolation considered herein are 1) increase in safety (or reduction in risk), and 2) a reduction in OCC and the cost of SSCs. The GNF is populated with SSCs commonly employed in US nuclear facilities. The GNF is sited at INL and LANL. Two variants of the GNF are analysed: conventionally founded and base isolated. The target isolation period is approximately 2 seconds.

Seismic probabilistic risk assessment (SPRA) is performed using the five-step methodology proposed by Huang et al. (2011a, 2011b). Two procedures are used to assess system functionality: 1) a new simplified procedure based on Boolean algebra, and 2) a more rigorous Monte Carlo procedure. The values of mean annual frequency of unacceptable performance, namely, the loss of MAR, calculated using the two procedures, are similar at a given site (i.e., INL or LANL) and base condition (i.e., conventionally founded or base-isolated). The simplified Boolean-based method appears to be a viable risk calculation tool for use in the early stages of a nuclear-facility design.

The mean annual frequency of unacceptable performance decreases by many orders of magnitude with the implementation of seismic isolation at the INL and LANL sites. The required seismic ruggedness (and cost) of the SSCs in the isolated GNF can be decreased significantly and still easily achieve the target performance goals expected of nuclear facilities in the United States.

The cost benefits of isolation are assessed using data from Stevenson (1981, 2003). Calculations of the overnight capital cost (OCC) and the cost of SSCs, as a function of the intensity of earthquake shaking are made for the conventionally founded and base-isolated GNFs. The results of these cost calculations indicate that seismic base isolation would reduce the OCC of the GNF at both INL and LANL, with greater reductions at LANL.

ACKNOWLEDGMENTS

This study was funded by the US Department of Energy, Office of Nuclear Energy. The authors are grateful for this financial support.

REFERENCES

- American Society of Civil Engineers (ASCE). (2005). "Seismic design requirements for structures, systems and components in nuclear facilities," *ASCE/SEI Standard 43-05*, Reston, VA, USA.
- American Society of Civil Engineers (ASCE). (2010). "Minimum design loads for buildings and other structures," *ASCE/SEI Standard 7-10*, Reston, VA, USA.
- American Society of Civil Engineers (ASCE). (2016). "Seismic analysis of safety-related nuclear structures and commentary," *ASCE/SEI Standard 4-16*, Reston, VA, USA.
- Bolisetti, C., Yu, C.-C., Coleman, J., Kosbab, B., and Whittaker, A. S. (2016). "Characterizing the benefits of seismic isolation to nuclear facilities: a framework for risk-based decisions making," *INL/EXT-16-40122*, Idaho National Laboratory, Idaho Falls, ID, USA.
- Electric Power Research Institute (EPRI). (2013). "Seismic probabilistic risk assessment implementation guide," *3002000709*, Palo Alto, CA, USA.
- Federal Emergency Management Agency (FEMA). (2012). "Seismic performance assessment of buildings, Volume 1 - methodology," *FEMA P-58-1*, Washington, D.C., USA.
- Hancock, J., Watson-Lamprey, J., Abrahamson, N. A., Bommer, J. J., Markatis, A., McCoy, E., and Mendis, R. (2006). "An improved method of matching response spectra of recorded earthquake ground motion using wavelets," *Journal of Earthquake Engineering*, 10 (spec01), 67-89.
- Huang, Y.-N., Whittaker, A. S., Kennedy, R. P., and Mayes, R. L. (2009). "Assessment of base-isolated nuclear structures for design and beyond-design basis earthquake shaking," *MCEER-09-0008*, University at Buffalo, The State University of New York, Buffalo, NY, USA.
- Huang, Y.-N., Whittaker, A. S., and Luco, N. (2011a). "A seismic risk assessment procedure for nuclear power plants, (I) methodology," *Nuclear Engineering and Design*, 241, 3996-4003.
- Huang, Y.-N., Whittaker, A. S., and Luco, N. (2011b). "A seismic risk assessment procedure for nuclear power plants, (II) application," *Nuclear Engineering and Design*, 241, 4004-4011.
- Livermore Software Technology Corporation (LSTC). (2013). *LS-DYNA keyword user's manual - Version R 7.0*, Livermore, CA, USA.
- Reed, J. W., and Kennedy, R. P. (1994). "Methodology for developing seismic fragilities," *TR-103959*, Electric Power Research Institute, Palo Alto, CA, USA.
- Stevenson, J. D. (1981). "Evaluation of the cost effects on nuclear power plant construction resulting from the increase in seismic design level," *NUREG/CR-1508*, United States Nuclear Regulatory Commission, Washington, D.C., USA.
- Stevenson, J. D. (2003). "Historical development of the seismic requirements for construction of nuclear power plants in the U.S. and worldwide and their current impact on cost and safety," *Transactions, 17th International Conference on Structural Mechanics in Reactor Technology (SMiRT-17)*, Prague, Czech Republic.
- Yu, C.-C., Bolisetti, C., Coleman, J., Kosbab, B., and Whittaker, A. (2017). "Using seismic isolation to reduce risk and capital cost of safety-related nuclear structures," Paper submitted for review and possible publication, *Nuclear Engineering and Design*.
- Yu, C.-C., and Huang, Y.-N. (2017). "An improved methodology for Monte Carlo-based seismic probabilistic risk assessment of a nuclear power plant," Paper submitted for review and possible publication, *Nuclear Engineering and Design*.
- Yang, T. Y., Moehle, J. P., Stojadinovic, B., and Der Kiureghian, A. (2009). "Performance evaluation of structural systems: theory and implementation," *Journal of Structural Engineering*, 135(10), 1146-1154.